

 **Mini-Circuits®**



Connecting  Mini-Circuits & Israel


2019

NEW PRODUCT GUIDE

Local Technical Support:
admin1@mcdi-ltd.com
077-5406075
www.mcdi-ltd.com



NPG19Q4

TABLE OF CONTENTS

4	10	30
6	16	34
14	32	44

- ADAPTERS
- AMPLIFIERS
- CABLES
- COUPLERS
- FILTERS
- SPLITTERS/COMBINERS
- SWITCHES
- TRANSFORMERS
- DESIGNER'S KITS

ADAPTERS

HIGHLIGHTS

- New NMD 2.92mm and 2.4mm adapters facilitate connections to lab instrumentation
- New 1.85mm adapters up to 67 GHz

AD

ADAPTERS

50Ω DC to 40 GHz

NMD 2.92mm and 2.4mm Adapters

- Facilitates direct connection to lab instrumentation
- Ultra-wideband
- Flat response
- Low insertion loss
- Excellent VSWR



Model Number	Conn. 1	Conn. 1	Frequency Range	VSWR
KF-24MNM+	2.92mm-F	2.4mm NMD-M	DC-40	1.06
KFNMD-24MNM+	2.92mm NMD-F	2.4mm NMD-M	DC-40	1.08
KFNMD-KMNM+	2.92mm NMD-F	2.92mm NMD-M	DC-40	1.05
KM-24MNM+	2.92mm-M	2.4mm NMD-M	DC-40	1.04
KMNM-24MNM+	2.92mm NMD-M	2.4mm NMD-M	DC-40	1.06

50Ω DC to 67000 MHz

1.85mm Adapters

- Flat response
- Low insertion loss
- Excellent VSWR



Model Number	Conn. 1	Conn. 1	Frequency Range (MHz)	VSWR
185F-185F+	1.85mm-F	1.85mm-F	DC-67000	1.05
185M-185F+	1.85mm-M	1.85mm-F	DC-67000	1.04
185M-185M+	1.85mm-M	1.85mm-M	DC-67000	1.04
185F-24F+	1.85mm-F	2.4mm-F	DC-50000	1.08
185F-24M+	1.85mm-F	2.4mm-M	DC-50000	1.08
185M-24F+	1.85mm-M	2.4mm-F	DC-50000	1.06
185M-24M+	1.85mm-M	2.4mm-M	DC-50000	1.04
185F-KF+	1.85mm-F	2.92mm-F	DC-40000	1.05
185F-KM+	1.85mm-F	2.92mm-M	DC-40000	1.04
185M-KF+	1.85mm-M	2.92mm-F	DC-40000	1.04
185M-KM+	1.85mm-M	2.92mm-M	DC-40000	1.03

AMPLIFIERS

HIGHLIGHTS

- ▶ New Ultra-Wideband Coaxial Amplifiers up to 43.5 GHz
- ▶ New MMIC amplifiers with low noise and high dynamic range
- ▶ Wideband class A/AB amplifiers up to 5W

50Ω 0.05 to 43500 MHz
Ultra-Wideband Coaxial Amplifiers

- Ultra-wideband
- Excellent gain flatness
- Rugged designs feature built-in protections against over-voltage, reverse voltage, and in-rush current



NEW RELEASES	Frequency Range (MHz)	Gain (dB) Typ.	NF (dB) Typ.	P1dB (dBm) Typ.	OIP3 (dBm) Typ.	Voltage (V)	DC Current (mA)
Model Number							
ZVA-24443G1+	24000-43500	45	1.7	20	27	15	160
ZVA-02443HP+	2000-43500	37	3.5	17	25	15	130
ZVA-443HGX+	10-43500	33	3.5	9	18	15	225
ZVA-443X+	0.05-43500	11	4.5	10	22	5	80
ZVE-403-K+	26000-40000	22	9	19	21	12	300
ZVA-403GX+	0.05-40000	11	4.5	11	21	5	100
ZVE-323LN-K+	18000-32000	20	3	10	23	12	50
ZVA-203GX+	1500-21000	29	3	15.5	27.5	5	450
ZVA-213-S+	800-21000	26	3	24	33	12	400
ZX60-06203LN+	6000-20000	18.4	2.8	15.6	27.4	5	128
ZX60-24-S+	5000-20000	24	6.8	18	27	5	260
ZX60-24A-S+	5000-20000	24	6.4	18.3	25.4	5	27
ZX60-022203+	2000-20000	21.5	6.5	14.6	28	5	155
ZVA-213UWX+	100-20000	14	3	16	29	+12, -5	84
ZX60-183-S+	6000-18000	23.5	6.9	18.1	27.2	5	260
ZX60-183A-S+	6000-18000	28	5	18	27	5	260
ZX60-06183LN+	6000-18000	25	2.1	11	24	5	64
ZVA-183-S+	700-18000	26	3	24	33	12	400
ZVA-183G-S+	500-18000	38	3	25	36	15	770
ZVA-183W-S+	100-18000	28	3	26	34.5	15	625
ZX60-153LN-S+	500-15000	16	2.8	15	27	12	82
ZX60-14012L-S+	0.3-14000	12	5.5	11	20	12	62
ZX60-123LN-S+	500-12000	17	2.4	16	28	12	82
ZX60-05113LN+	5000-11000	21.4	1.9	13	24.5	5	42
ZX60-83LN-S+	500-8000	22.1	1.4	20.7	35.2	5/6	60/70

50Ω DC to 18000 MHz
MMIC Amplifiers

- Wideband
- Low Noise
- High dynamic range



Model Number	Frequency Range (MHz)	Gain (dB)	NF (dB)	P1dB (dBm)	OIP3 (dBm)	Voltage (V)	DC Current (mA)	Case Style
PMA2-183LN+	4000-18000	10.4	2.5	14.2	25.6	5	48.2	2x2mm QFN
PHA-83W+	50-8000	15.7	3.3	23.3	35.5	5.0/9.0	41/110	SOT-89
PSA-39+	DC-6000	23	2.2	10.7	23.3	5	32	SOT-363
PSA-8A+	DC-4000	31	3	12.8	25.8	5	36	2x2mm QFN

50Ω 0.0025 to 6000 MHz
Wideband Coaxial Class A/AB Amplifiers

- Wideband
- High gain, up to 45 dB
- Excellent linearity



Model Number	Frequency Range (MHz)	Gain (dB)	NF (dB)	P1dB (dBm)	OIP3 (dBm)	Voltage (V)	DC Current (mA)	Connector Type
ZHL-1W-63-S+	600-6000	35	12	30	35	15	1000	SMA
ZHL-1W-63X-S+	600-6000	35	12	30	35	15	1000	SMA
ZHL-2W-63-S+	600-6000	42	12	33	38	28	2000	SMA
ZHL-5W-63-S+	600-6000	45	12	37	42	28	3500	SMA
ZHL-6A+	0.0025-500	25	9.5	22	34	24	350	BNC
ZHL-6A-N+	0.0025-500	25	9.5	22	34	24	350	N
ZHL-6A-S+	0.0025-500	25	9.5	22	34	24	350	SMA

CABLES

HIGHLIGHTS

- ▶ Flexible interconnect cables
- ▶ Ultra-flexible precision test cables

50Ω DC to 40000 MHz
Flexible Interconnect Cables

- Flexible construction
- Ideal for integrating coaxial components and subassemblies
- Excellent return loss and insertion loss



NEW RELEASES	Frequency Range (MHz)	Center Diameter (IN)	Length (FT)	Conn. 1	Conn. 2	Insertion Loss (dB)
Item Number						
FL086-3KM+	DC-40000	0.086	0.25	2.92mm-M	2.92mm-M	0.5
FL086-4KM+	DC-40000	0.086	0.33	2.92mm-M	2.92mm-M	0.6
FL086-6KM+	DC-40000	0.086	0.5	2.92mm-M	2.92mm-M	0.9
FL086-12KM+	DC-40000	0.086	1.0	2.92mm-M	2.92mm-M	1.5
FL086-6-35M+	DC-30000	0.086	0.5	3.5mm-M	3.5mm-M	0.7
FL086-12-35M+	DC-30000	0.086	1.0	3.5mm-M	3.5mm-M	1.29
FL086-6NM+	DC-18000	0.086	0.5	N-Type-Male	N-Type-Male	0.3
FL086-6SM+	DC-18000	0.086	0.5	SMA-Male	SMA-Male	0.4
FL086-6SMNM+	DC-18000	0.086	0.5	N-Type-Male	SMA-Male	0.3
FL086-9SM+	DC-18000	0.086	0.75	SMA-Male	SMA-Male	0.64
FL086-12NM+	DC-18000	0.086	1.0	N-Type-Male	N-Type-Male	0.6
FL086-12SM+	DC-18000	0.086	1.0	SMA-Male	SMA-Male	0.9
FL086-12SMNM+	DC-18000	0.086	1.0	N-Type-Male	SMA-Male	0.7
FL086-24NM+	DC-18000	0.086	2.0	N-Type-Male	N-Type-Male	1.4
FL086-24SM+	DC-18000	0.086	2.0	SMA-Male	SMA-Male	1.5
FL086-24SMNM+	DC-18000	0.086	2.0	N-Type-Male	SMA-Male	1.4
FL141-6NM+	DC-18000	0.141	0.5	N-Type-Male	N-Type-Male	0.2
FL141-6SM+	DC-18000	0.141	0.5	SMA-Male	SMA-Male	0.3
FL141-6SMNM+	DC-18000	0.141	0.5	N-Type-Male	SMA-Male	0.2
FL141-9SM+	DC-18000	0.141	0.75	SMA-Male	SMA-Male	0.37
FL141-12NM+	DC-18000	0.141	1.0	N-Type-Male	N-Type-Male	0.4
FL141-12SM+	DC-18000	0.141	1.0	SMA-Male	SMA-Male	0.5
FL141-12SMNM+	DC-18000	0.141	1.0	N-Type-Male	SMA-Male	0.4
FL141-24NM+	DC-18000	0.141	2.0	N-Type-Male	N-Type-Male	0.9
FL141-24SM+	DC-18000	0.141	2.0	SMA-Male	SMA-Male	1.0
FL141-24SMNM+	DC-18000	0.141	2.0	N-Type-Male	SMA-Male	0.9

50Ω DC to 18000 MHz
Flexible Test Cables

- Minimal performance change vs. flexure
- Tight bend radius, 2.0"
- Booted joints protect the connector interface during bending
- Excellent return loss and insertion loss



NEW RELEASES	Frequency Range (MHz)	Length (FT)	Conn. 1	Conn. 2	Insertion Loss (dB)
Item Number					
ULC-10FT-NMNM+	DC-18000	10.0	N-Type-Male	N-Type-Male	7.0
ULC-10FT-SMSM+	DC-18000	10.0	SMA-Male	SMA-Male	7.5
ULC-8FT-SMSM+	DC-18000	8.0	SMA-Male	SMA-Male	5.4
ULC-6FT-NMNM+	DC-18000	6.0	N-Type-Male	N-Type-Male	4.6
ULC-6FT-SMNM+	DC-18000	6.0	N-Type-Male	SMA-Male	4.4
ULC-6FT-SMSM+	DC-18000	6.0	SMA-Male	SMA-Male	5.2
ULC-4FT-NMNM+	DC-18000	4.0	N-Type-Male	N-Type-Male	4.0
ULC-4FT-SMNM+	DC-18000	4.0	N-Type-Male	SMA-Male	3.1
ULC-4FT-SMSM+	DC-18000	4.0	SMA-Male	SMA-Male	3.4
ULC-1M-NMNM+	DC-18000	3.28	N-Type-Male	N-Type-Male	2.6
ULC-1M-SMNM+	DC-18000	3.28	N-Type-Male	SMA-Male	2.5
ULC-1M-SMSM+	DC-18000	3.28	SMA-Male	SMA-Male	2.8
ULC-3FT-NMNM+	DC-18000	3.0	N-Type-Male	N-Type-Male	2.2
ULC-3FT-SMNM+	DC-18000	3.0	N-Type-Male	SMA-Male	2.2
ULC-3FT-SMSM+	DC-18000	3.0	SMA-Male	SMA-Male	2.7
ULC-2FT-NMNM+	DC-18000	2.0	N-Type-Male	N-Type-Male	1.6
ULC-2FT-SMNM+	DC-18000	2.0	N-Type-Male	SMA-Male	1.5
ULC-2FT-SMSM+	DC-18000	2.0	SMA-Male	SMA-Male	1.8
ULC-1.5FT-SMSM+	DC-18000	1.5	SMA-Male	SMA-Male	1.4
ULC-1FT-SMSM+	DC-18000	1.0	SMA-Male	SMA-Male	0.7

COUPLERS

H I G H L I G H T S
► Ultra-wide bandwidth, now up to 50 GHz

CO

COUPLERS

50Ω 500 MHz to 50 GHz
Ultra-Wideband Directional Couplers

- Ultra-wide bandwidth, now up to 50 GHz
- Excellent coupling flatness
- Good directivity
- DC passing



NEW RELEASES	Frequency Range (MHz)	Coupling (dB) Nom.	Mainline Loss (dB)	Directivity (dB)	VSWR (:1)	Power Input Max. (W)
Model Number						
ZCDC30-K1844+	18000-40000	30	0.6	22	1.15	20
ZCDC30-K0644+	6000-40000	30	0.5	22	1.12	20
ZCDC30-18263-S+	18000-26500	30	0.6	21	1.14	20
ZCDC30-06263-S+	6000-26500	30	0.6	23	1.12	20
ZCDC30-02263-S+	2000-26500	30	0.6	23	1.14	20
ZCDC30-01263-S+	1000-26500	30	0.8	23	1.14	20
ZCDC30-5R263-S+	500-26500	30	0.6	28	1.07	20
ZCDC20-K1844+	18000-40000	20	0.7	19	1.17	20
ZCDC20-K0644+	6000-40000	20	0.7	22	1.07	20
ZCDC20-K0244+	2000-40000	20	1.0	20	1.17	20
ZCDC20-K0144+	1000-40000	20	1.2	20	1.20	20
ZCDC20-18263-S+	18000-26500	20	0.4	24	1.14	20
ZCDC20-06263-S+	6000-26500	20	0.5	26	1.14	20
ZCDC20-02263S+	2000-26500	20	0.5	18	1.33	20
ZCDC20-01263-S+	1000-26500	20	0.9	23	1.12	20
ZCDC20-5R263-S+	500-26500	20	0.9	25	1.09	20
ZCDC16-K1844+	18000-40000	16	0.7	23	1.10	20
ZCDC16-K0244+	2000-40000	16	1.2	20	1.19	20
ZCDC16-K0144+	1000-40000	16	1.3	20	1.22	19
ZCDC16-K5R44W+	500-40000	16	2.0	19	1.19	20
ZCDC16-02263-S+	2000-26500	16	0.6	26	1.09	20
ZCDC16-01263-S+	1000-26500	16	0.9	21	1.14	20
ZCDC16-5R263-S+	500-26500	16	1.4	23	1.12	20
ZCDC13-K26344+	26500-40000	13	0.9	21	1.22	20
ZCDC13-K1844+	18000-40000	13	0.9	21	1.13	20
ZCDC13-K0244+	2000-40000	13	0.95	24	1.11	20
ZCDC13-K0144+	1000-40000	13	1.5	19	1.73	13
ZCDC13-01263-S+	1000-26500	13	1.2	21	1.17	19
ZCDC13-5R263-S+	500-26500	13	1.3	21	1.73	20
ZCDC10-V254+	2000-50000	10	1.3	23	1.08	13
ZCDC10-K1844+	18000-40000	10	1.2	21	1.22	17
ZCDC10-K0644+	6000-40000	10	1.0	24	1.12	17
ZCDC10-K0244+	2000-40000	10	1.2	23	1.11	15
ZCDC10-K0144+	1000-40000	10	2.2	16	1.22	19
ZCDC10-K5R44W+	500-40000	10	1.3	23	1.12	15
ZCDC10-18263-S+	18000-26500	10	0.9	24	1.15	20
ZCDC10-06263-S+	6000-26500	10	1.0	22	1.17	20
ZCDC10-02263S+	2000-26500	10	0.9	27	1.11	20
ZCDC10-01263-S+	1000-26500	10	0.9	21	1.17	20
ZCDC10-5R263-S+	500-26500	10	1.2	22	1.12	20

FILTERS

HIGHLIGHTS

- ▶ LTCC Balun Filters
- ▶ New Cavity Filters
- ▶ Application Note: Filtering without Reflections

FL

FILTERS

50Ω 2400 to 2500 MHz

LTCC Balun-Filters

- Integrated balun and bandpass filter in a single 0805 monolith
- Band-optimized for Wi-Fi, Bluetooth and Zigbee

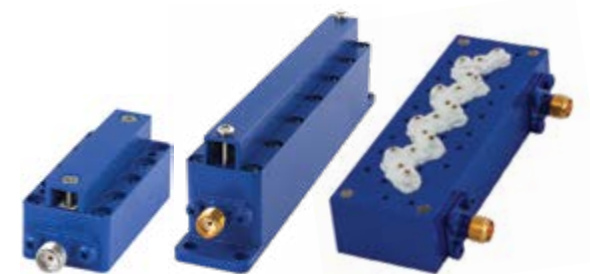


Model Number	Passband (MHz)	Stopband F3 (MHz)	Rejection @ F3 (dB)	Stopband F4 (MHz)	Rejection @ F4 (dB)
BFGE2-552R+	4900-5875	DC-3500	49	-	-
BFGE1-252R+	2400-2500	1000-2000	39	4800-5000	49
BFNL2-252R+	2400-2500	1710-1910	38	4800-5000	42

50Ω 902 to 11400 MHz

Cavity Bandpass Filters

- Passbands as narrow as 1%
- Very low passband insertion loss
- Very fast roll-off with wide stopband
- High power handling, up to 15W



NEW RELEASES					
Model Number	Passband (MHz)	Stopband F3 (MHz)	Rejection @ F3 (dB)	Stopband F4 (MHz)	Rejection @ F4 (dB)
ZVBP-11G3-S+	11200-11400	DC-11030	35	11580-20000	35
ZVBP-10R5G-S+	9750-11250	DC-5950	35	15100-18000	35
ZVBP-9R6G-S+	9550-9650	DC-9300	30	9900-20400	33
ZVBP-8250-S+	8025-8475	DC-7650	20	8925-11000	20
ZVBP-7100-S+	7025-7175	DC-6990	36	7224-14000	35
ZVBP-5800-S+	5725-5875	DC-5200	35	6400-14000	35
ZVBP-5310-S+	5250-5370	DC-5080	20	5530-8250	20
ZVBP-4900-S+	4840-4960	DC-4670	20	5100-9000	20
ZVBP-4810-S+	4750-4870	DC-4600	20	5020-8250	20
ZVBP-4300-S+	4250-4350	DC-4140	20	4480-8000	20
ZVBP-4000-S+	3997-4003	DC - 3800	70	4200 - 6000	70
ZVBP-3875-S+	3845-3905	DC-3785	35	3970-8500	35
ZVBP-2450-S+	2400-2500	2120-2260	40	2635-2780	40
ZVBP-2400-S+	2375-2425	DC-2250	35	2550-6000	35
ZVBP-2300A-S+	2200-2400	DC-2000	30	2550-8050	30
ZVBP-2072R5-S+	2030-2115	DC-1930	48	2220-6000	49
ZVBP-1420-N+	1415-1425	DC-1370	81	1470-3000	79
ZVBP-909-S+	902-915	10-895	20	925-2300	20
ZVBP-909A-S+	902-915	DC-895	27	923-2300	35

FILTERING WITHOUT REFLECTIONS:

Flattening Multiplier Chain Conversion Efficiency & More

Rohan Shrotriya, Mini-Circuits Applications
Dr. Matthew A. Morgan, National Radio Astronomy Observatory

ABSTRACT

A new class of filter, which exhibits broadband matched impedance at its ports, has recently been invented and made available. This new device, the reflectionless filter, has demonstrated a variety of benefits when used to replace conventional filters in a signal chain. This white paper briefly introduces the reflectionless filter and compares conventional filter and reflectionless filter behavior. Use cases are presented examining how reflectionless filters can improve system performance when used with mixers, ADCs, and receiver signal chains. Lastly, an experiment is described and test results presented to compare the conversion loss ripple in multiplier chains when reflectionless and reflective filters are used to filter spurious signals.

INTRODUCTION

The advent of broad bandwidth amplifiers, analog-to-digital converters (ADCs), digital-to-analog converters (DACs), and software-defined radios has brought about growing interest in broadband communications, radar, and sensing applications. For these applications, there is often a need to preserve the highest sensitivity and dynamic range possible within the receiver signal chain and to mitigate the number and strength of harmonics and spurious content in the transmitter signal chain. This is a substantial challenge considering the nature of non-linear components within these circuits, namely compression-mode amplifiers, mixers, multipliers, and frequency-conversion electronics.

A long-overlooked opportunity to enhance the signal-to-noise ratio (SNR) and dynamic range within a signal chain and to reduce harmonics/spurious content within these circuits is to address a seemingly innate property of filters: their out-of-band reflective behavior. Reflectionless filters utilize a novel circuit topology to effectively eliminate the standing waves created by traditional filters without additional components (such as pads). This unique property gives designers a new way to improve the system performance of a wide array of broadband circuits, or any circuits suffering from out-of-band impedance mismatch.

REFLECTIONLESS FILTER BASICS

A Brief History of the Genesis of Reflectionless Filters

Reflectionless filters were born from a desire to enhance the signal chain performance of sensitive radio astronomy receivers. Innovators of the technology noted that the typical performance of conventional filters (reflective filters) only exhibited a matched impedance at its ports within the filter’s pass-band. The stop-band regions of these filters are intentionally designed to have very poor impedance match. As a result, undesired stop-band signals, including harmonics, interference, and noise, are all reflected from the filter ports back through the signal chain. If these unwanted signals are reflected back to another reflective device, a standing wave effect emerges. This standing wave will persist and build on itself until the attenuation of the transmission path between the two reflective components dampens and absorbs the unwanted signal energy.

In the case of non-linear devices (amplifiers, mixers, converters, etc.), this standing wave can lead to a number of undesirable effects including:

- Gain compression
- Oscillations
- Proliferation of spurious mixing products
- Unexpected resonances
- Degraded stability
- Degraded dynamic range
- Greater susceptibility to process tolerances/environmental factors
- Biasing issues

Hence, it is often necessary to insert isolators or attenuators (pads) into the signal path to dampen this standing wave effect. However, neither isolators nor pads are an ideal solution for most applications. Isolators are band-limited devices with a large footprint, while attenuators are broadband absorbers that absorb even pass-band signal energy. The increased insertion loss from either of these methods may lead to the need for additional gain in the system, and both solutions add cost, size, complexity, and failure points to the circuit.

A better solution is to design a filter that absorbs signal energy in the stop-band instead of reflecting it. Though absorptive filter technologies have existed for some time, their design and implementation didn’t meet all of the desired criteria for a true conventional filter replacement. Hence, a ground-up design effort culminated in the birth of the reflectionless filter, which is a set of filter topologies and designs that inherently exhibit a broadband matched impedance.

Overview of Reflectionless Filter Theory

Reflectionless filter topologies are often realized as symmetric networks. This enables the use of even-/odd-mode analysis techniques, which aids in understanding the reflectionless nature of these filters. Given a two-port network with a perfect symmetry plane dividing the circuit, there are two modes useful for analysis. The even mode occurs when both ports are stimulated by signals of equal amplitude and phase, which means there is no current passing across the symmetry plane. The odd mode occurs when the signals stimulated at either port are equal in amplitude and opposite in phase (180 degrees out of phase), and where the voltage potential at the nodes along the symmetry plane is 0 referenced to ground.

Under these conditions, two separate single-port networks can be drawn, each with only half the elements of the original two-port network with the nodes along the symmetry plane either shorted to ground or open (odd-mode circuits and even-mode circuits). Hence, the scattering parameters of the two-port network can be derived from the superposition of the reflection coefficients of the two circuits detailed in Equations 1 and 2.

Equation 1

$\Gamma_{even} = s_{11} + s_{12} = s_{22} + s_{21} \text{ \& } \Gamma_{odd} = s_{11} - s_{12} = s_{22} - s_{21}$

Equation 2

$s_{11} = s_{12} = \frac{1}{2}(\Gamma_{even} + \Gamma_{odd}) \text{ \& } s_{21} = s_{12} = \frac{1}{2}(\Gamma_{even} - \Gamma_{odd})$

Given the S-parameters, a condition of exact input match ($S_{11} = S_{22} = 0$) can be derived from Equation 3. This condition can only be satisfied if the even-mode and odd-mode circuits are duals of each other (i.e. where their reflection coefficients are additive inverses of one another), which means that the inductors and capacitors, along with the series and shunt elements within each circuit are swapped compared to the other. The result of the combined circuit is a transfer function for the original two-port network equivalent to the reflection coefficient of the even-mode circuit.

Equation 3

For $s_{11} = s_{22} = 0$, $s_{21} = s_{12} = \Gamma_{even} = \Gamma_{odd}$

Therefore, low-pass, high-pass, band-pass, and band-stop filters can be generated by choosing a filter topology whose reflection characteristic matches the desired transfer characteristic (even-mode circuit), creating a dual of the chosen filter topology (odd-mode circuit), performing topological modifications that result in symmetry between the even-/odd-mode circuits without affecting the circuit behavior, then combining the two circuit-halves to form the final two-port filter network (See Figure 1 and 2).

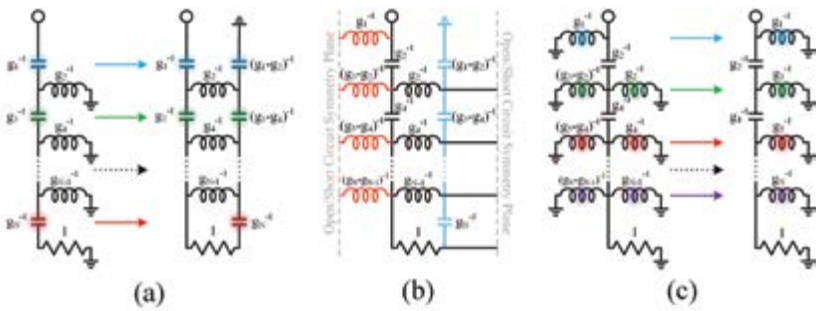


Figure 1: (a) A ladder topology high-pass filter is converted to an even-mode equivalent circuit for a low-pass reflectionless filter. (b) The inductors in red are eliminated in the open circuit case and the capacitors in blue are eliminated during a short circuit case when the plane of symmetry is opened/shorted to develop the odd-mode equivalent circuit from the even mode equivalent circuit. (c) The odd-mode equivalent circuit is developed from the short-circuit case and simplified.

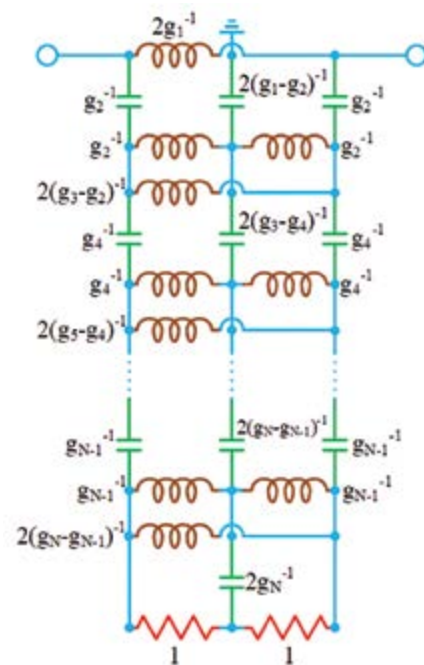
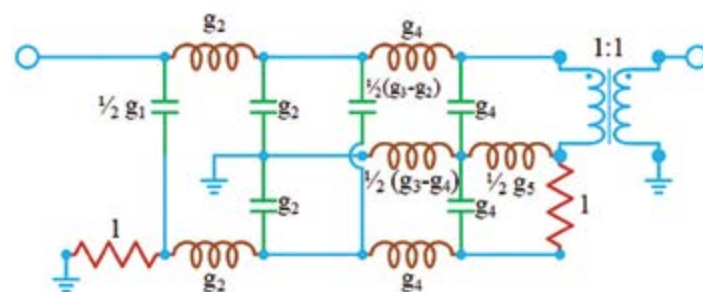


Figure 2: An Nth order high-pass reflectionless filter circuit based on even-odd mode synthesis.

It is important to note that for some filter responses, such as Chebyshev, the filter ripple is bounded by the need to maintain positive element values (unless a modification is applied which requires the use of transformers [6]). Hence, for these types of filters there is an additional limit to the stop-band rejection, which means the stop-band rejection only reaches approximately 13-14 dB and is somewhat dependant on the order of the filter. Therefore, when using these filter types to design reflectionless filters it may be necessary to cascade several filters or use a filter response less encumbered by this restriction (i.e. Zolotarev response).

Figure 3: An example 5th order Chebyshev type 1 reflectionless filter.



A Note on Practical Reflectionless Filters

In their current incarnation, reflectionless filters have been mass-produced using a gallium arsenide (GaAs) semiconductor Integrated Passive Device (IPD) fabrication process (see Figure 4). Reflectionless filters with frequency response from hundreds of megahertz to over 30 gigahertz have been realized [9, 10]. A benefit of the GaAs IPD process is that the resulting reflectionless filters are also extremely stable over temperature and exhibit a relatively high operating temperature beyond 100 degrees C.



Figure 4: A compact Reflectionless Filter package built using a gallium arsenide (GaAs) passive device process.

As with any practical filter, additional loss and parasitics do affect performance relative to the ideal filter circuit. In the case of the GaAs IPD process, the extremely small filters are built with equally compact and planar spiral inductors and capacitors, which have relatively low Q values. Hence, the tradeoff for extremely compact size (3x3 QFN package) and excellent repeatability in these filters is generally greater characteristic insertion loss. However, a benefit of the reflectionless filter topology is that these filters are readily cascadable, so sharper roll-off and greater stop-band rejection may be achieved by adding filters as modular building blocks.

This cascadability allows designers to combine reflectionless filters to achieve a desired response. For example, reflectionless filters may be cascaded to enhance a filter's stop-band attenuation, extend the stop-band match, or create ultra-wideband (UWB) filters. The examples plotted in Figure 5 show that the stop-band attenuation, which is ultimately limited by the fabrication constraints of the GaAs IPD process, can be improved by combining two complementary low-pass reflectionless filters. Moreover, Figure 6 illustrates that a UWB band-pass filter with good stop-band match can be achieved by combining a low-pass and a high-pass reflectionless filter.

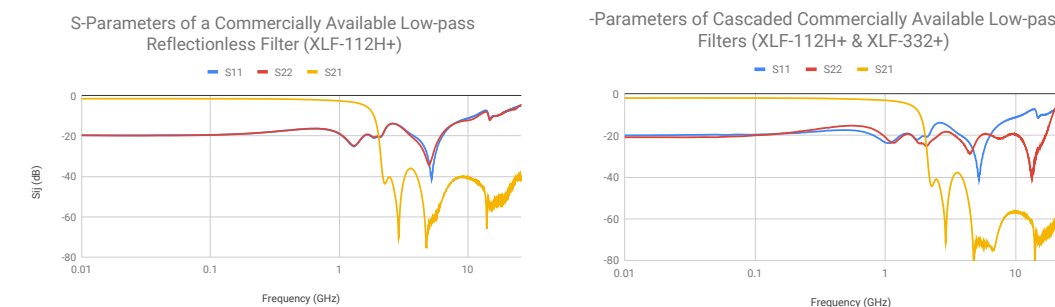


Figure 5: S-Parameters of a single reflectionless low-pass filter versus two cascaded reflectionless low-pass filters

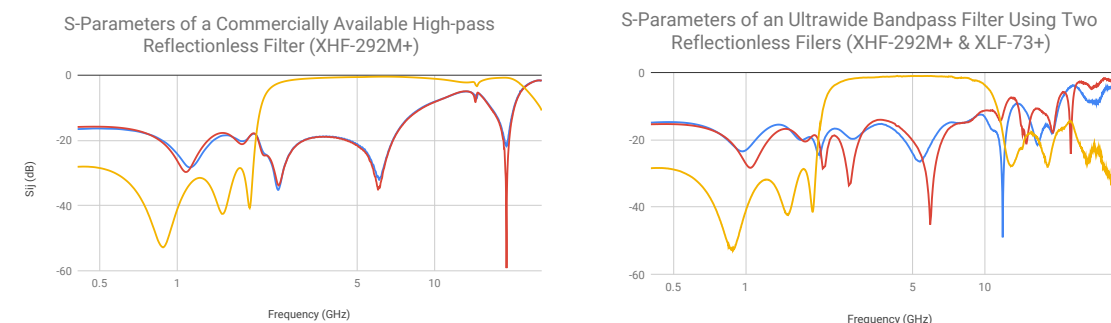


Figure 6: A UWB band-pass filter with good stop-band match can be realized by combining a low-pass and a high-pass reflectionless filter.

REFLECTIONLESS FILTERS VERSUS CONVENTIONAL FILTERS

It is easy enough to understand the value of having pass-band and stop-band matched impedance at each port of a filter in concept, but it is more instructive to see practical results of the difference between reflective and reflectionless filters in specific implementations. The following examples and discussion revolve around the effects of cascading both reflective and reflectionless filters. Here we examine the negative performance impacts of poor impedance match, compared to filters that are matched at every frequency.

Whereas cascading conventional filters can lead to ripple and cause phase instability in the pass-band, these same concerns are not applicable to reflectionless filters. For example, when comparing conventional filters with reflectionless filters in series, the cascaded conventional filter response will likely suffer from increased ripple in the stop-band due to an unstable phase relationship between the through and reflected signal. Moreover, a conventional filter will also suffer from additional pass-band ripple as a product of the resulting reflections in the transition. Cascading reflectionless filters, by contrast, eliminates the distortion and additional ripples common to conventional filters, but creates an expected accumulation of insertion loss (see Figure 7) [10].

Figure 7: Cascading conventional filters increases ripple in the stop-band and passband. Reflectionless filters eliminated this unwanted effect but introduce an expected accumulation of insertion loss.

When cascaded, conventional reflective filters also suffer degradation of input and output return loss of the transition

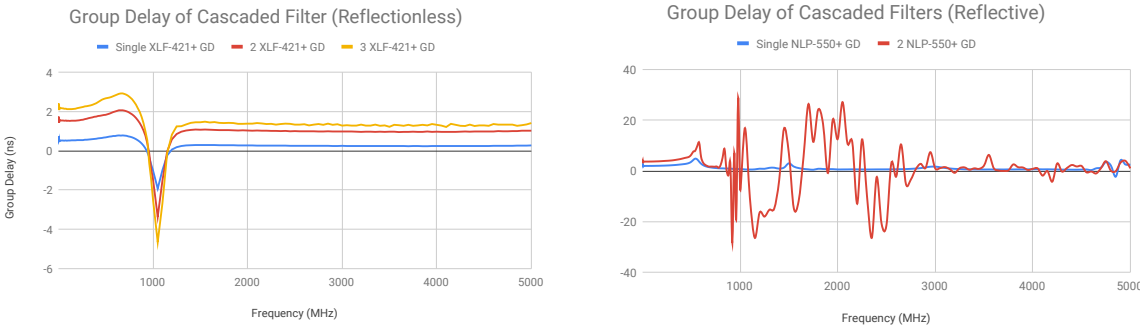


corner response due to their poor match in the transition. For example, Figure 8 compares the input and output return loss of cascaded reflective and reflectionless filters. The input and output return loss of just two conventional filter sections in cascade varies significantly around the cutoff frequency. By contrast, the three-section cascaded reflectionless filter exhibits relatively consistent input and output return loss in the pass-band to stop-band transition. This example indicates that where cascading conventional filters degrades the filter’s frequency response (i.e. passband performance), cascading reflectionless filters simply adds a predictable amount of insertion loss without other unwanted effects.

Lastly, the reactive impedance of a conventional filter tends to result in distortion and phase instability, which worsens as filter sections are added. These performance degradations directly impact the group delay performance of conventional cascaded filters (see Figure 9) [10]. Cascaded reflectionless filters, on the other hand, exhibit relatively flat group delay through the pass-band, transition, and stop-band.

Figure 8: Comparison of output return loss of cascaded reflective and reflectionless filters.

Figure 9: Comparison of group delay of cascaded reflectionless and reflective filters.



REFLECTIONLESS FILTER USE CASES

The following section discusses several applications where replacing conventional filters with reflectionless filters can improve overall system response. Finally, a detailed experiment is presented to illustrate the use of reflectionless filters in multiplier chains and related benefits for system performance.

Pairing with Mixers (Up-/Down-converters) To Improve SNR and Dynamic Range

One inherent aspect of a mixer’s non-linear behavior is the creation of undesirable leakage and spurious signals in various areas of the spectrum (images and etc.). Filters are often used to help suppress these unwanted mixer products (see Figure 10). However, at the ports of a mixer, a conventional filter’s stop-band reactive impedance can degrade dynamic range and conversion loss. It can also lead to the development of nulls and increase sensitivity to process variations, phase instability, amplitude instability, expansion of the intermodulation products, and more. Replacing a conventional filter with a reflectionless filter in an anti-aliasing or image rejection application can improve sideband separation, enhance calibration longevity, and mitigate mixer sensitivities to process tolerances. Moreover, a reflectionless filter and mixer pair (if the reflectionless filter is well chosen for the specific mixer) exhibits nearly the same IP3 performance as the mixer alone, which is not the case for conventional filters. Therefore, replacing a conventional filter with a reflectionless filter may allow the use of a mixer with lower intrinsic IP3 while still meeting system specifications, or at least avoid the need for a mixer with higher IP3 to meet the same system specifications.

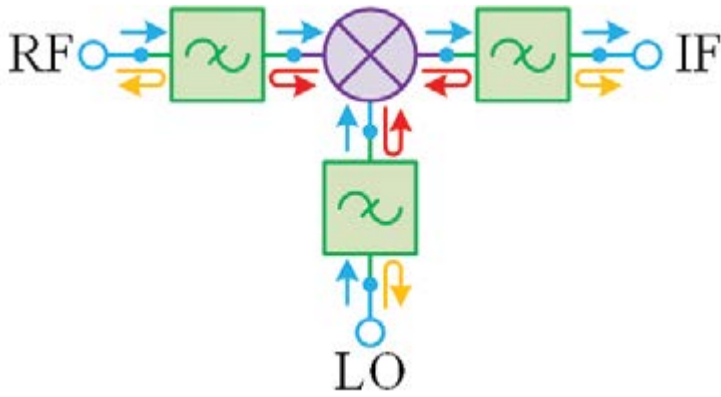


Figure 10: Using conventional (reflective) filters generates reflections and standing waves from out-of-band signals at each port of the conventional filters. Signal path for reflectionless filters shown in blue. Signal reflections created by conventional filters shown in red and yellow.

Wideband ADC Antialiasing Filter

During the sample-and-hold or track-and-hold operations of an ADC, the switching action of the input stage creates a rapid change in the load conditions for the driving circuit. These switching transients may also generate pulses that back-propagate through the system. Though intended for this purpose, the switching transients and other non-linear products may occur at frequencies well beyond the anti-aliasing filter's operating frequency range. As these filters aren't intended to be true broadband devices, the impedance matching at these higher frequencies may be poor enough to yield reflections of the switching transients and non-linear products back to the ADC input, create a standing wave and otherwise impact the ADC's output performance (spur-free dynamic range and noise figure).

In this case, reflectionless filters can be employed at the input of the ADC to absorb the out-of-band signals and mitigate the effect of switching transients. Reflectionless filters can be added to both differential inputs of the ADC, eliminating differential and common-mode switching transients (see Figure 11). If greater selectivity is required than what the typical MMIC reflectionless filters can offer, a traditional anti-aliasing filter with higher Q elements or a cascaded reflectionless filter could be added in series.

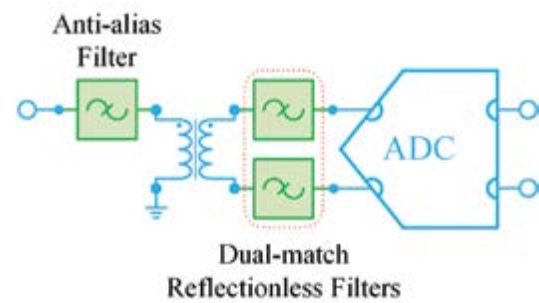


Figure 11: Block diagram depicting how a dual-matched reflectionless filter can be used to improve ADC anti-alias filtering.

Optimizing Receiver Sensitivity and Dynamic Range with a Distributed Filter Approach

Optimizing a receiver signal chain is essential to achieving the desired sensitivity and dynamic range for the system. As is often the case with RF circuits, there is generally a trade-off between sensitivity and dynamic range when attempting to filter out-of-band signals.

Filtering prior to amplifying the received signal attenuates the out-of-band noise and interference, improving dynamic range. However, this approach also attenuates the strength of the received signal, which reduces the overall receiver sensitivity. Placing the filter after the amplifier allows for greater sensitivity, but reduces dynamic range. It may therefore be desirable to distribute filters with a minimal amount of insertion loss throughout the signal chain.

Unfortunately, cascading conventional (reflective) filters isn't viable as the out-of-band interactions between the filters can further degrade signal quality. Reflectionless filters, however, can be cascaded without any undesirable side-effects. Hence, a new modular approach of cascading reflectionless filters throughout a signal chain to reach the desired level of sensitivity and dynamic range becomes possible (see Figure 12).

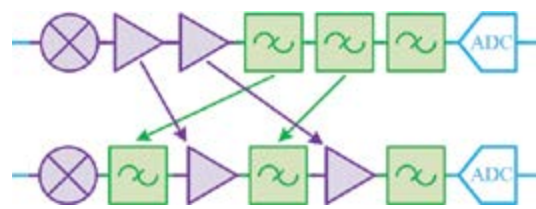


Figure 12: Block diagram representing the process of distributing filters throughout a signal chain to optimize response.

Multipliers and Multiplier Chains: Stabilizing Conversion Efficiency over Frequency

EXPERIMENT

Frequency translation devices such as multipliers and dividers are used to convert frequencies from lower spectrum regimes to higher frequencies, and vice versa. As these devices are intrinsically non-linear, they generate spurious harmonics, which are often filtered to prevent harmonics from appearing in-band. Using conventional, reflective filters creates an undesirable scenario where the out-of-band harmonics are reflected back to the multiplier. The multiplier is also affected by the reactive loading exhibited by a reflective filter at harmonic frequencies (see Figure 13). Given that multipliers have poor output return loss, this combination of effects leads to large ripples in the conversion efficiency of a multiplier chain, and hence, susceptibility to environmental factors.

As discussed earlier, this issue can be solved by leveraging the unique capabilities of reflectionless filters. In order to demonstrate this solution, an experiment was conducted with a doubler test circuit and a 4X multiplier chain. Each experiment was conducted using comparable reflective and reflectionless filters, and the results were then analyzed (see Figure 14).

The tests were conducted using an Agilent E8257D PSG signal generator and an Agilent U2000A power meter. The doubler used in all tests was a Mini-Circuits ZX90-2-36-S+. The second doubler was a KSX2-24+. The amplifier used in the multiplier chain was a GALI-39+. The conventional filter was a Mini-Circuits VLF-6400+, and the reflectionless filter was a Mini-Circuits XLF-662M+. Each test was done using four different lengths of interconnect between the connectorized doubler and filter: no cable, a 6-inch coaxial cable, a 12-inch coaxial cable, and a 36-inch coaxial cable. An image of the test setup of the doubler-filter pair is presented in Figure 15.

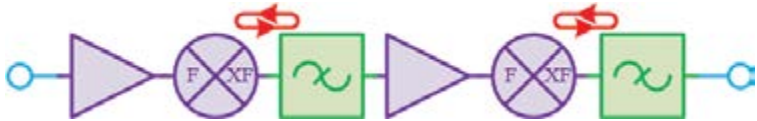


Figure 13: The reflections that develop into standing waves in a multiplier chain occur at the output of the multipliers and the input of the conventional reflective filters.

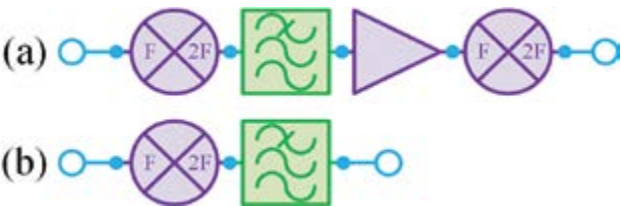


Figure 14: (a) A diagram of the experimental multiplier chain block diagram. (b) A diagram of the experimental signal chain.



Figure 15: (top) A reflectionless filter and doubler pair. (bottom) A reflective filter and doubler pair.

RESULTS

Results of the two experiments are shown in Figures 16, 17, 18, and 19. Figure 16 shows the conversion loss of a doubler-filter pair at various power levels with a reflectionless filter (left) and a reflective filter (right). It can be observed from the plots in Figure 16, that even at nominal power levels for the doubler, the reflective filter's out-of-band impedance mismatch leads to reflections of the harmonics, especially the 3rd harmonic, which leads to greater conversion loss ripple. Figure 17 exaggerates this point by replicating the experiment that produced Figure 16 with a longer transmission line length between the filter and doubler by 6 inches, allowing for a greater development of standing waves. Figure 17 shows that the reflectionless filter (left) is able to effectively attenuate the out-of-band reflections with almost no additional conversion loss ripple, while the reflective filter exhibits much worse standing wave effects the longer the transmission line used.

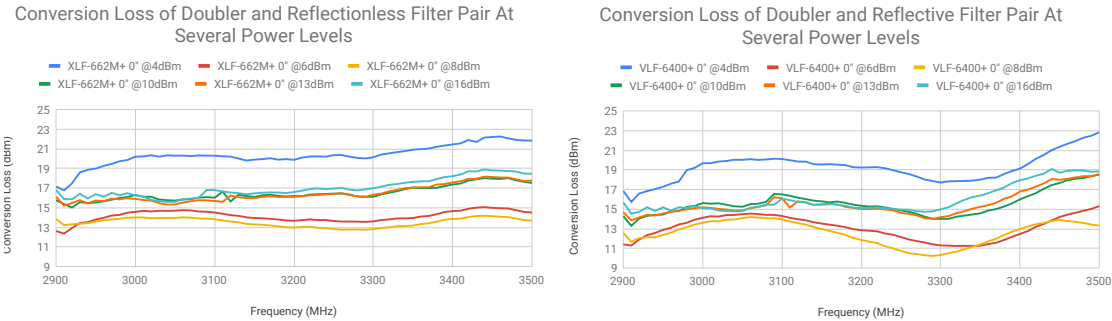


Figure 16: Conversion loss of a doubler-filter pair at various power levels. Reflectionless filter (left); Reflective filter (right).

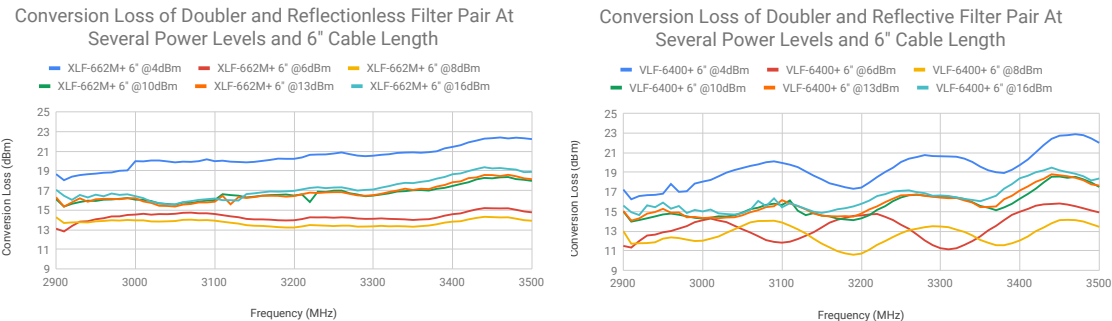


Figure 17: Conversion loss of doubler-filter pair with 6-inch cable length between the filter and doubler. Note the increased transmission length leads to greater development of standing waves.

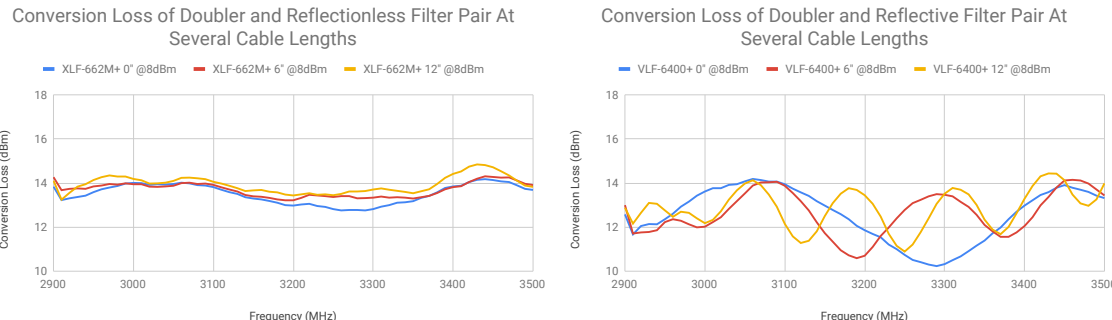


Figure 18: Conversion loss curves for doubler-filter pairs with conventional and reflectionless filters, illustrating effects of out-of-band impedance mismatch on standing waves in the signal chain.

Figure 18 captures the susceptibility of a doubler-filter pair to effects that can worsen the standing waves developed by filters with out-of-band impedance mismatch. Even in the worst case experimental example (a 36" transmission line extension), the reflectionless filter (left) only develops a marginal conversion loss ripple, while the ripple of the reflective filter (right) is over 2 dB. A side-by-side comparison of the conversion loss ripple for both the reflective and reflectionless filter is provided in Figure 19.

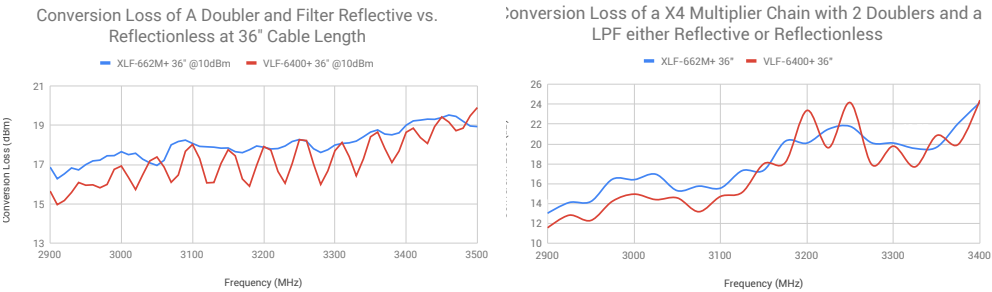


Figure 19: Side-by-side comparisons of conversion loss ripple for a doubler-filter pair (left) and X4 multiplier chain with a filter after the first doubler (right) when conventional and reflectionless filters are used.

Lastly, in Figure 19 (right) an X4 multiplier chain is tested using two doublers with a filter after the first doubler. This plot shows that the conversion loss ripple under worst-case conditions (extended transmission line) is greater for the reflective filter than the reflectionless filter by over 3 dB peak-to-peak. In order to achieve comparable conversion loss ripple with a conventional filter to that of a reflectionless filter, a much higher power amplifier and an extra attenuator would be necessary to push the doublers well into saturation and mitigate the standing wave generated by the higher power level. In longer multiplier chains, the reflective nature of conventional filters may degrade conversion loss flatness even further and require careful selection of amplifiers and attenuators distributed throughout the multiplier chain, adding size, cost and complexity to the system. By contrast, a well-chosen amplifier with a reflectionless filter can achieve flat conversion loss efficiency while minimizing cost, size and the need for extra components.

CONCLUSION

This white paper has reviewed the basic genesis and theory of reflectionless filters, compared conventional reflective filters and reflectionless filter technology (both theoretically and practically), and described several applications that may benefit from replacing conventional filters with reflectionless filters. An experimental example was also described in detail and test results analyzed to illustrate the benefits of using reflectionless filters with multipliers and in multiplier chains. This discussion has shown several ways that reflectionless filters can overcome many of the typical design challenges associated with introducing reflective filters into a signal chain, and in particular the development of standing waves from stop-band signals due to the reactive loading of reflective filters. Reflectionless filters have become a valuable new tool in the RF/microwave engineer's toolbox, and future developments of reflectionless filter technology may yield even higher performing filtering solutions.

REFERENCES

1. M. Morgan, "A better way to filter -- part I," NRAO Blog, March 29, 2018.
2. M. Morgan, Reflectionless Filters, Norwood, MA: Artech House, January 2017.
3. Hong J, (ed.). Advances in Planar Filters Design. Institution of Engineering and Technology, 2019. 424 p.
4. Morgan, M. A., & Boyd, T. A. (2011). Theoretical and Experimental Study of a New Class of Reflectionless Filter. IEEE Transactions on Microwave Theory and Techniques, 59(5), 1214-1221. doi:10.1109/tmtt.2011.2113189
5. Morgan, M. A., & Boyd, T. A. (2015). Reflectionless Filter Structures. IEEE Transactions on Microwave Theory and Techniques, 63(4), 1263-1271. doi:10.1109/tmtt.2015.2403841
6. Morgan, M. A., Groves, W. M., & Boyd, T. A. (2018). Reflectionless Filter Topologies Supporting Arbitrary Low-Pass Ladder Prototypes. IEEE Transactions on Circuits and Systems I: Regular Papers, 1-11. doi:10.1109/tcsi.2018.2872424
7. M. Morgan, "Think Outside the Band: Design and Miniaturization of Absorptive Filters," IEEE Microwave Magazine, vol. 19, no. 7, pp. 54-62, November 2018.
8. R. Setty, B. Kaplan, M. Morgan, and T. Boyd, "Combining MMIC Reflectionless Filters to Create UWB band-pass Filters," Microwave Journal, vol. 61, no. 3, pp. 60-72, March 2018.
9. Pairing Mixers with Reflectionless Filters to Improve System Performance, Mini-Circuits Application Note
10. Advantages of Cascading Reflectionless Filters, Mini-Circuits Application Note
11. M. Morgan, "Reflectionless Filters," U.S. Patent No. 8,392,495, March 5, 2013. People's Republic of China Patent No. 201080014266.1, July 30, 2014.
12. M. Morgan, "Optimal Response Reflectionless Filters," U.S. Patent No. 10,263,592, April 16, 2019. Taiwan Patent No. I653826, March 11, 2019.
13. M. Morgan, "Transmission Line Reflectionless Filters," U.S. Patent No. 9,923,540, March 20, 2018, No. 10,277,189, April 30, 2019.

REFLECTIONLESS FILTERS KEY FEATURES

1. Ideal for broadband systems sensitive to out-of-band standing waves
2. Enable integration of wideband amplifiers without creating out-of-band instabilities
3. May be cascaded to create UWB filters
4. Ideal for cases where stop-band signals present significant harmonics or interference affecting the source
5. Reduce BOM by replacing filter/attenuator pairs (absorbers)
6. Ideal where stable performance over temperature is desirable
7. High operating temperature allows for placement close to high-power components

SPLITTERS/ COMBINERS

SC

SPLITTERS/COMBINERS

50Ω DC to 43500 MHz

Ultra-Wideband MMIC Splitter/Combiners

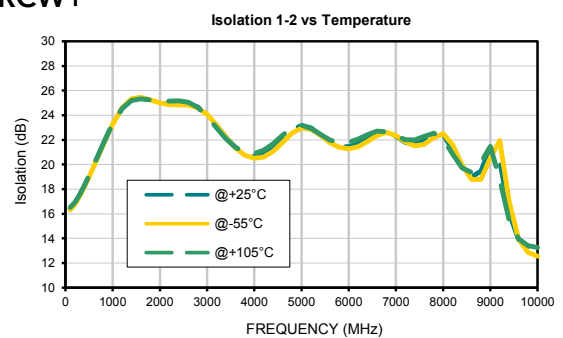
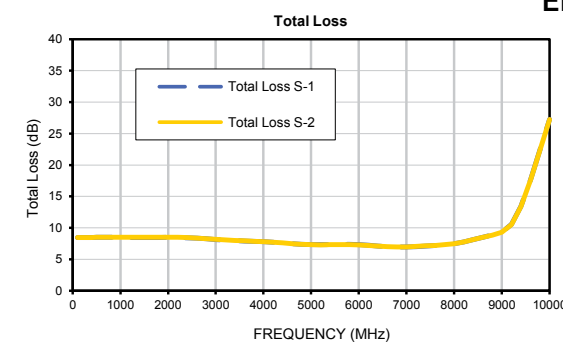
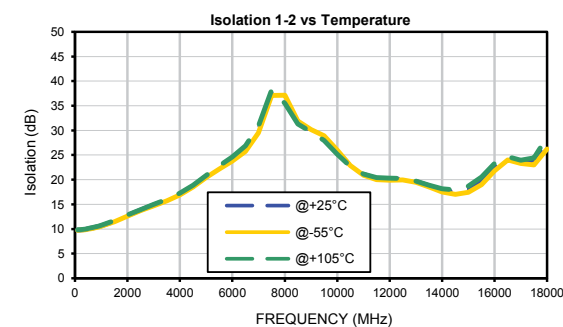
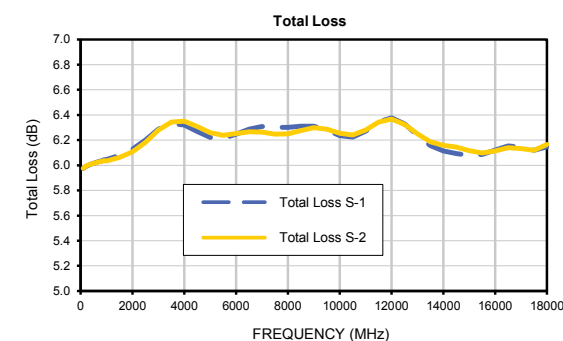
- Power handling up to 2.5W
- Low insertion loss
- Excellent isolation
- New resistive/reactive designs extend frequency coverage down to DC



NEW RELEASES		No. of Ways	Frequency Range (MHz)	Isolation (dB)	Insertion Loss (dB)	Phase Unbalance (deg)	Amplitude Unbalance (dB)	Power Input (W) as Splitter, Max.	DC Pass
Model Number									
EP2KA+		2	10000-43500	17	2.2	9.6	0.57	1.25	Y
EP4KA+		4	10700-31000	19.3	0.6	4.7	0.2	0.6	Y
EP2K1+		2	2000-26500	20	2.4	5.4	0.3	2.5	Y
EP2K+		2	5000-20000	20	2.1	4.2	0.1	2.5	Y
EP2RKU+		2	DC-18000	26.1	3.3	1.1	0.02	0.3	N
EP4RKU+		4	DC-18000	18.8	3.8	1.9	0.2	0.6	N
EP2C+		2	1800-12500	16	1.1	6	0.2	1.85	Y
EP2W1+		2	500-9500	19.4	1.8	1.7	0.1	2.5	Y
EP2RCW+		2	DC-8000	23.0	4.8	0.9	0.02	0.3	N
EP2W+		2	700-6000	19.8	1.3	0.9	0.1	2.5	Y

HIGHLIGHTS

- Ultra-wideband MMIC splitter/combiners
- New resistive/reactive designs extend frequency coverage down to DC



SWITCHES

- H I G H L I G H T S**
- New wideband MMIC switches provide high isolation and fast switching speed.

SW

SWITCHES

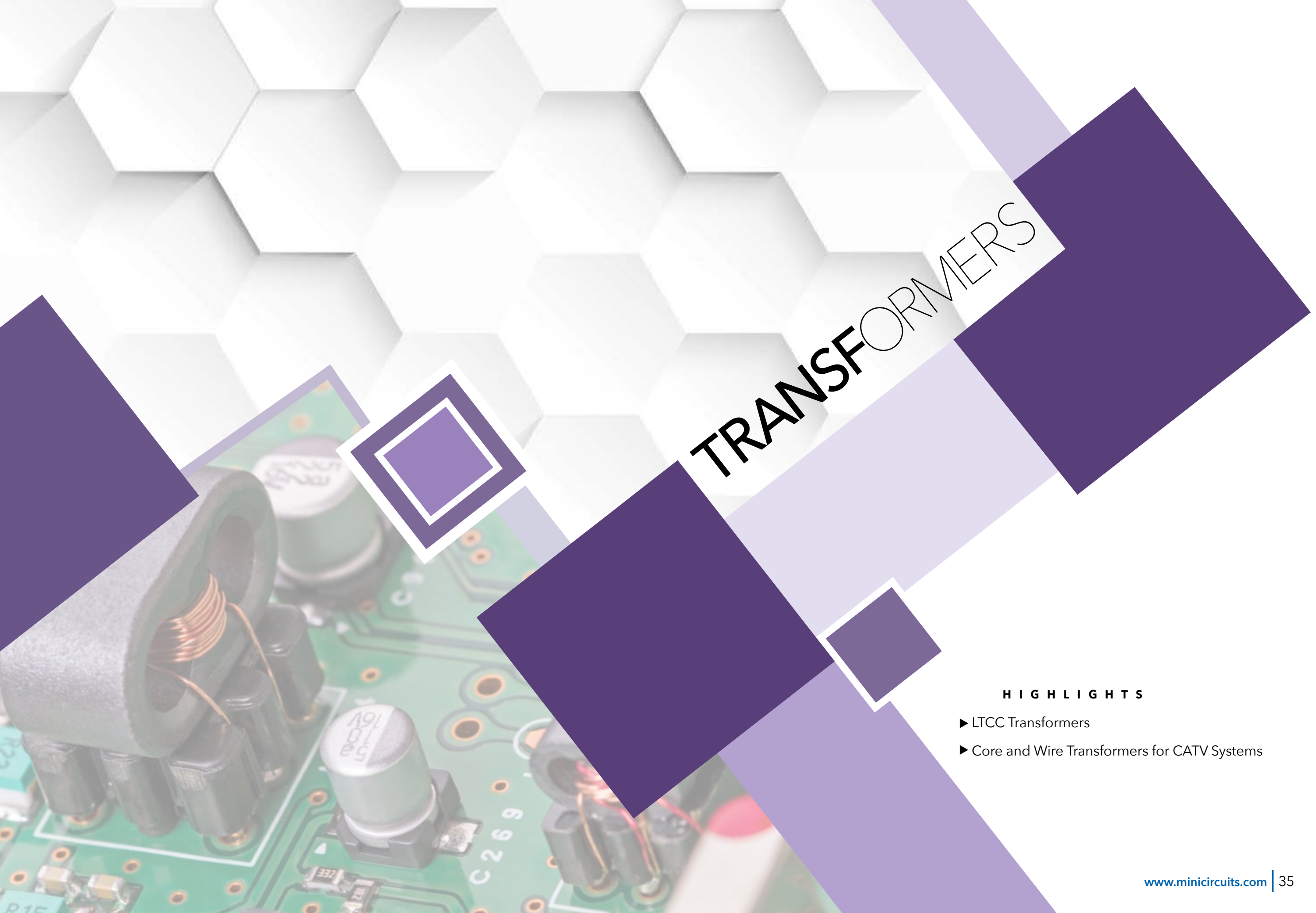
50Ω DC to 6000 MHz

MMIC Switches

- Fast switching
- Excellent isolation
- With and without internal CMOS drivers
- Tiny size, as small as 2x2mm



NEW RELEASES									
Model Number	Type	Frequency Range (MHz)	Driver	Configuration	Insertion Loss (dB)	1 dB Compression (dBm)	Input IP3 (dBm)	In-Out Isolation (dB)	
CSWA2-63DR+	SPDT	500-6000	CMOS	Absorb	1.1	27	45	50	
VSWA2-63DR+	SPDT	500-6000	CMOS	Absorb	1.2	27	44	46	
HSWA2-63DR+	SPDT	100-6000	CMOS	Absorb	1	35	65	68	
HSWA4-63DR+	SP4T	30-6000	CMOS	Absorb	1.15	35	58	52	
JSW2-63DR+	SPDT	5-6000	CMOS	Reflect	0.33	35	59	35	
JSW2-63VHDRG+	SPDT	5-6000	CMOS	Reflect	0.36	37	75	33	
JSW2-63VHDRP+	SPDT	5-6000	CMOS	Reflect	0.36	37	75	33	
MSW2-50+	SPDT	DC-5000	-	Reflect	0.7	23	54	53	
MSWA2-50+	SPDT	DC-5000	-	Absorb	0.7	24	54	53	
M3SW-2-50DRA+	SPDT	DC-4500	CMOS	Reflect	0.6	25	47.3	48	
M3SWA-2-50DRA+	SPDT	500-4500	CMOS	Absorb	1.2	27	46	51	
M3SWA-2-50DRB+	SPDT	DC-4500	CMOS	Absorb	0.6	25.4	46.5	56	
VSW2-33-10W+	SPDT	50-3000	-	Reflect	0.5	40	56	26	
HSWA2-30DR+	SPDT	DC-3000	CMOS	Absorb	0.9	31	55	55	
HSW2-272VHDR+	SPDT	30-2700	CMOS	Reflect	0.4	45.5	85	28	
JSW3-272DR+	SP3T	5-2700	CMOS	Reflect	0.6	35	59	30	
JSW4-272DR+	SP4T	5-2700	CMOS	Reflect	0.6	35	59	30	
JSW5-272DR+	SP5T	5-2700	CMOS	Reflect	0.6	35	59	30	
JSW6-33DR+	SP6T	5-2700	CMOS	Reflect	0.6	35	59	30	
MSW-2-20+	SPDT	DC-2000	-	Reflect	0.5	24	-	34	
MSWA-2-20+	SPDT	DC-2000	-	Absorb	0.95	27	-	40	



TRANSFORMERS

H I G H L I G H T S

- ▶ LTCC Transformers
- ▶ Core and Wire Transformers for CATV Systems

50Ω & 75Ω 223 to 8000 MHz

LTCC Baluns

- Tiny size, 0805
- Excellent power handling
- Rugged ceramic construction
- Cost effective for volume production



NEW RELEASE	Frequency Range (MHz)	Single-Ended to Single-Ended	Single-Ended to Balanced	Balanced to Balanced	Center Tap	DC Isolation	Impedance (Ω)	Impedance Ratio
Model Number								
NCS2-83+	3000-8000	N	Y	N	N	Y	50	2
NCS2-622+	5600-6200	N	Y	N	N	Y	50	2
NCS1-63+	4900-6000	N	Y	N	N	Y	50	1
NCS4-63+	4500-6000	N	Y	N	N	Y	50	4
NCS2-592+	4900-5875	N	Y	N	N	Y	50	2
NCS4-442+	3300-4200	N	Y	N	N	Y	50	2
NCS1-422+	3300-4000	N	Y	N	N	Y	50	1
NCS2-392+	3000-3900	N	Y	N	N	Y	50	2
NCS1-332+	700-3300	N	Y	N	N	Y	50	1
NCS2-33+	1500-3100	N	Y	N	N	Y	50	2
NCS1-292+	1650-2850	N	Y	N	N	Y	50	1
NCS3-272+	2250-2725	N	Y	N	N	Y	50	3
NCS4-272+	2300-2700	N	Y	N	N	Y	50	4
NCS4-232+	1600-2300	N	Y	N	N	Y	50	4
NCS2-232+	900-2300	N	Y	N	N	Y	50	2
NCS1.5-232+	400-2300	N	Y	N	N	Y	50	1.5
NCS2-222+	1275-2200	N	Y	N	N	Y	50	2
NCS2-222-2+	1275-2200	N	Y	N	N	Y	50	2
NCS1-222-75+	950-2200	N	Y	N	N	Y	75	1
NCS1-23+	1300-2000	N	Y	N	N	Y	50	1
NCS1-112+	700-1100	N	Y	N	N	Y	50	1
NCS4-102+	700-1000	N	Y	N	N	Y	50	4
NCS2-771+	240-770	N	Y	N	N	Y	50	2
NCS2-771-75+	240-770	N	Y	N	N	Y	75	2
NCS3-72+	250-760	N	Y	N	N	Y	50	3
NCS2-62+	390-590	N	Y	N	N	Y	50	2
NCS1-521+	223-520	N	Y	N	N	N	50	1
NCS4-521+	223-520	N	Y	N	N	Y	50	4

75Ω 4.5 to 3000 MHz

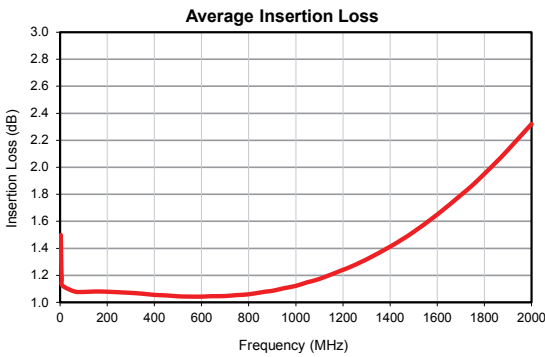
Core and Wire Transformers for CATV

- Broadband, supporting DOCSIS® 3.1 and 4.0 bandwidth requirements

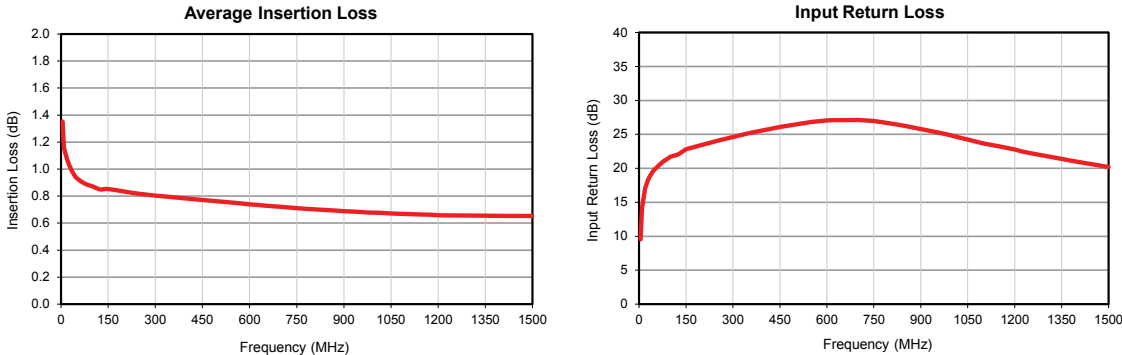


NEW RELEASES	Frequency Range (MHz)	Single-Ended to Single-Ended	Single-Ended to Balanced	Balanced to Balanced	Center Tap	DC Isolation	Impedance Ratio
Model Number							
SCTX1.33-33-2W+	10-3000	N	Y	N	N	N	1.33
TC1-33-75G2+	5-3000	N	Y	Y	N	N	1
TC1-1-13M-75+	4.5-3000	N	Y	Y	N	N	1
TC1-1-13M-75X+	4.5-3000	N	Y	Y	N	N	1
TRS1-23-75+	10-2200	N	Y	Y	N	N	1
TRS1-182-75+	10-1800	N	Y	Y	N	N	1
TC1.33-182X-75+	5-1800	N	Y	N	Y	N	1.33
TCM2-142-75X+	10-1400	N	Y	Y	N	N	2
TRC1-1K122-75+	20-1250	N	Y	Y	N	N	1
TRC1-1-122-75+	5-1250	N	Y	N	N	N	1

TC1.33-182X-75+



TRC1-1K122-75+



DEMYSTIFYING RF TRANSFORMERS

Part 1: A Primer on Transformer Theory, Technologies, and Applications

William Yu and Urvashi Sengal, Mini-Circuits

INTRODUCTION

In essence, a transformer is merely two or more conductive paths linked by a mutual magnetic field. When a varying magnetic flux is developed within the core by alternating current passing through one conductive path, a current is then induced in the other conductive paths. This induced current is proportional to the ratio of magnetic coupling between the two conductive paths. The ratio of the magnetic coupling of the conductive paths with the core determines the induced voltage in the additional conductive paths, providing both an impedance transformation and a voltage step-up or step-down. Additional conductive paths, potentially all with different coupling ratios, may be added to realize various functions, which is why RF transformers are such varied and versatile devices used widely throughout the RF/microwave industry.

A common implementation of an RF transformer consists of two or more distinct wires wrapped around a magnetic core (or air core for higher frequencies), which is why RF transformers are often described as a ratio of the number of windings, or turns.

RF transformers are used for a wide variety of applications, as the nature of the device allows for various configurations that can serve a variety of different functions, including (but not limited to):

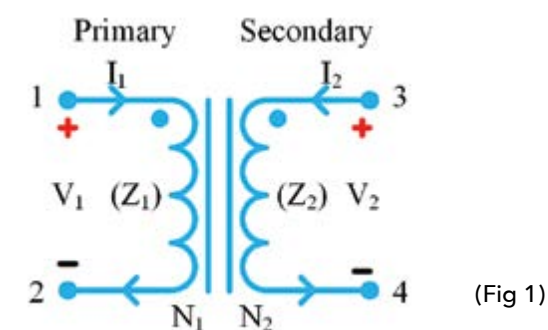
- Injecting DC current
- Providing DC isolation between circuits
- Enhancing common mode rejection
- Providing an impedance transformation for impedance matching
- Efficiently coupling between balanced and unbalanced circuits
- Inducing a voltage/current step-up or step-down

There are several common technologies used to build transformers, including core-and-wire, transmission line, low temperature co-fired ceramic (LTCC), and monolithic microwave integrated circuit (MMIC). Each comes in a variety of packages and with a wide range of performance characteristics.

This article is the first part in our Demystifying RF Transformers series, and focuses on introducing RF transformer theory with discussion of common RF transformer technologies and applications.

TRANSFORMER THEORY AND PRACTICAL INSIGHTS

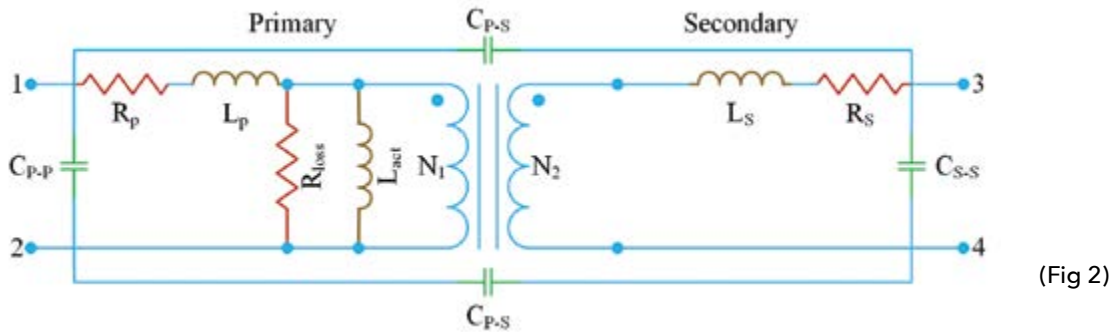
Though not viable for practical applications, the basic Ideal Transformer Model is helpful in illustrating the fundamental behavior of transformers. Consider the diagram, Figure 1. The current through the primary winding creates a magnetic flux (Faraday's Law) through the mutual magnetic field of the core, inducing a proportional current and voltage in the secondary winding. Both the current and voltage developed are proportional to the windings ratio, or magnetic coupling between the windings and the core.



Hence, the secondary impedance is a function of the square of the windings ratio times the impedance of the primary (Equation 1). Where I_1 , V_1 , and Z_1 are the current, voltage, and impedance through the primary winding; I_2 , V_2 , and Z_2 are the current, voltage, and impedance through the secondary winding, N_1 is the number of turns in the primary winding; N_2 is the number of turns in the secondary winding; 1 and 2 are the input ports of the primary winding; and lastly, 3 and 4 are the output ports of the secondary winding.

$$n = \frac{N_2}{N_1}, \quad V_2 = nV_1, \quad I_2 = \frac{I_1}{n}, \quad Z_1 = \frac{V_1}{I_1}, \quad Z_2 = \frac{V_2}{I_2}, \quad Z_2 = n^2 Z_1$$

However, a real transformer intrinsically includes several parasitic resistances, inductances, and capacitances, of which there are both mutual and self-parasitic capacitances. Illustrated in Figure 2 is a lumped-element model of a non-ideal transformer, which depicts parasitic resistances and inductances of the two windings, as well as core resistive losses and the windings' active inductance. It is clear from the model for a non-ideal transformer that these devices operate with a limited bandwidth, have insertion loss, a maximum power rating, and exhibit other frequency-, temperature- and power-dependent performance.



Typically, a real RF transformer’s lower cutoff frequency is dictated by the winding’s active inductance, and the high frequency cutoff is dominated by the inter-winding and intra-winding capacitance. Insertion loss present in the operating bandwidth is a product of the primary and secondary winding ohmic losses, as well as the dissipation within the core. As ohmic losses tend to be a function of frequency and temperature, the effective operating bandwidth of a transformer is limited by these factors. Several RF transformer types also introduce leakage inductances due to incomplete magnetic coupling between the windings. As the leakage inductance’s reactance is proportional to frequency, these parasitics reduce the return loss at high frequencies but increase the insertion loss at lower frequencies.

More complex RF transformer topologies, i.e. transformers with several windings, taps, and additional elements present varying performance dynamics based on the topology and transformer construction. For example, an RF device, known as a Balun, which is used to efficiently interconnect balanced (differential signal path) RF circuits to unbalanced (single-ended signal path) RF circuits using impedance transformation, can be realized with an RF transformer. Moreover, another device similar to a Balun, known as an Unun, which is used to interconnect unbalanced to unbalanced RF circuits, can also be realized with an RF transformer.

A common Balun fashioned from a transformer is a flux coupled Balun Transformer, which is constructed by winding separate wires around a magnetic core and grounding one side of the primary winding. Hence, the single-ended RF signals entering the primary unbalanced winding side undergo an impedance transformation to a differential (balanced) output through the secondary winding. A deeper examination of Balun and Unun theory, functions, and performance will be presented in Part 2 of the Demystifying RF Transformers series.

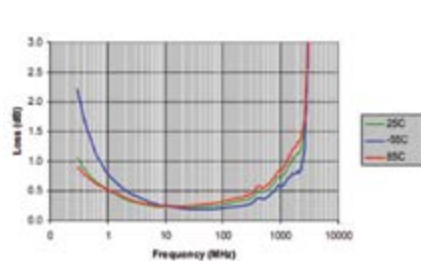


(Fig 3)

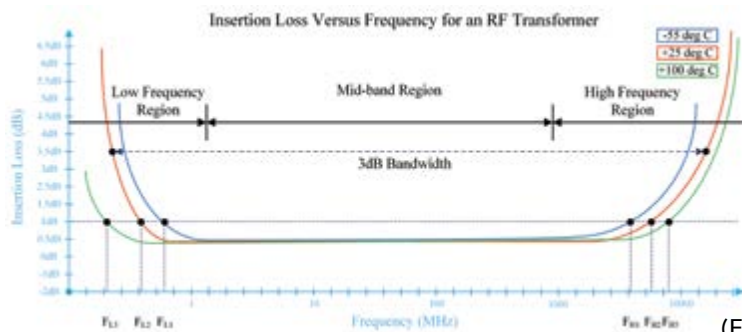


(Fig 4)

NOTES ON TRANSFORMER MAGNETIC CORES

RF transformers that include a magnetic core (typically ferromagnets) are subject to several undesirable performance degrading factors. For instance, the magnetizing inductance of the core limits the low frequency performance of an RF transformer. The magnetizing inductance is a function of the core permeability, cross sectional area of the magnetic core, and the number of windings around the core. The magnetizing inductance increases the insertion loss at low frequencies and also decreases the return loss. Furthermore, the permeability of the core is a function of temperature, for which increases in permeability subsequently increase the low frequency insertion loss.

RF TRANSFORMERS TECHNOLOGIES

The two main types of discrete RF transformers are core-and-wire and transmission line transformers. Additionally, there are two common types of low-profile and compact RF transformer designs: LTCC and MMIC transformers.

CORE-AND-WIRE RF TRANSFORMERS

Core-and-wire RF transformers are fabricated by wrapping conductive wires, typically insulated copper wires, around a magnetic core, such as a toroid. There may be one or more secondary windings, which may also be center tapped to enable additional functions. Figure 5 shows an RF transformer made from a toroidal magnetic core and insulated copper windings. Due to the nature of the inductive coupling between the wires and the core, smaller core and wire dimensions tend to yield core-and-wire transformers that can operate at much higher frequencies than larger core-and-wire transformers. However, the smaller dimensions of compact core-and-wire transformers also increase the resistive losses of the windings and the core, which exhibits greater insertion loss at lower frequencies.

TRANSMISSION LINE RF TRANSFORMERS

There are a variety of transmission line transformer topologies, which may include precisely designed transmission lines placed between two mismatched loads, or a complex arrangement of several transmission lines. For instance, a length of transmission line can be used to implement an impedance transformation between two mismatched loads. Some transmission line transformers use insulated wires wrapped around ferrite cores, which closely resemble typical core-and-wire transformers, and are often considered core-and-wire transformers. The following explanation is less for categorization purposes, but meant to describe aspects of transformer behavior and enhance understanding.



(Fig 5) Ideal transmission line transformer

A basic transmission line transformer consists of a two-conductor transmission line. The first conductor is connected from the generator to the load, and the other conductor is connected at the output of the first transmission line and the load to ground, as seen in Figure 6. With this configuration, the current flowing through the load is twice the current flowing through the generator, and V₀ is one half the voltage V₁. Hence, the load resistance is only a quarter of the resistance seen at the generator side, yielding a 1:4 transformer (Equation 2).

A common transmission line transformer variation is the quarter-wave transmission line transformer. This topology uses a transmission line with a characteristic impedance that enables impedance matching between the input impedance and the load. The length of a quarter-wave transformer is dictated by the desired frequency of operation, and is limited to one bandwidth octave around the center frequency. Consider a lossless transmission line with Z₀ characteristic impedance and length L, connected between Z_{in} input impedance and Z_L load impedance as seen in Figure 7. In order to match Z_{in} with Z_L, the characteristic impedance of the quarter-wave transmission line would need to be the square root of Z_{in} multiplied by Z_L (Equation 3).

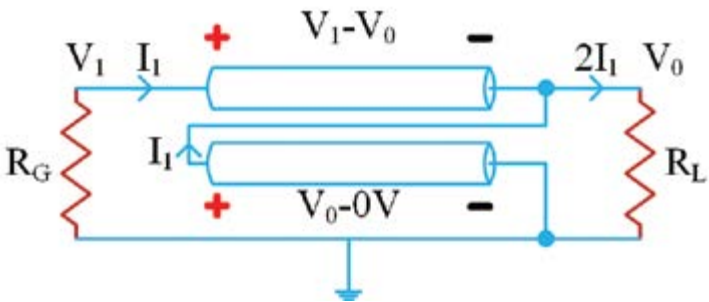


(Fig 6)

$$V_0 = \frac{V_1}{2}, R_G = \frac{V_1}{I_1}, R_L = \frac{V_0}{2I_1} = \frac{V_1/2}{2I_1} = \frac{R_G}{4} \quad (\text{Eq 2})$$

An advantage of a transmission line transformer is that a significant portion of the interwinding capacitance is assumed by the transmission line parameters, along with the leakage inductance, which results in a comparatively wider operating bandwidth compared to core-and-wire transformers.

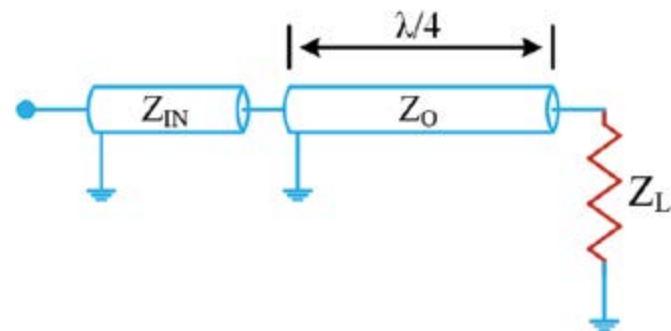


(Fig 7)

$$\beta = \frac{2\pi}{\lambda}, \quad Z_{IN} = Z_0 \frac{Z_L + jZ_0 \tan \beta L}{Z_0 + jZ_L \tan \beta L} \quad @ L \sim \frac{\lambda}{4} \quad Z_{IN} = \frac{Z_0^2}{Z_L}, \quad Z_0 = \sqrt{Z_{IN} Z_L} \quad (\text{Eq 3})$$

LTCC TRANSFORMERS

Low Temperature Co-fired Ceramic (LTCC) components are multilayer components that are fabricated using a ceramic-based substrate. LTCC transformers use coupled lines that act as transmission lines in order to achieve impedance transformation and signal conversion from single-ended to balanced. LTCC transformers rely on capacitive coupling to operate. This allows LTCC transformers to operate at higher frequencies compared to ferromagnetic transformers, but may lead to performance degradation at low frequencies. The benefit of LTCC technology is the ability to fabricate small and rugged transformers ideal for hi-rel applications, as seen in Figure 8.



(Fig8)

MMIC TRANSFORMERS

Like LTCC technologies, MMIC transformers are made using high-precision layered 2D substrates with planar metallization. Typically, MMIC transformers are fabricated using spiral inductors printed on a substrate in a two transmission line configuration parallel to each other. The MMIC process is helpful for producing high frequency transformers, and exhibits outstanding repeatability and excellent thermal efficiency. A MMIC transformer can be fabricated using gallium arsenide (GaAs) integrated passive device (IPD) process, as seen in Figure 9.



(Fig9)

INTRODUCTION TO RF TRANSFORMER FUNCTIONS & APPLICATIONS

As indicated in previous sections of this article, there are a variety of functions that RF transformers can perform depending upon their typology.

Transformation Functions

For instance, an impedance transformation function can be used to match two circuits with disparate impedance, or also provide a voltage step-up or step-down respective to a

Impedance Matching Transformers

There are many cases in RF circuits where a mismatch in impedances between two nodes can cause reduced power transfer efficiency and potentially troublesome reflections. Hence, an impedance matching transformer can be used to effectively eliminate the reflections and provide maximum power transfer between the two circuit nodes (see Figure 10).

Ununs and Baluns

Moreover, for unbalanced lines, an autotransformer configuration can be used for impedance matching, i.e. an Unun. As mentioned earlier, Balun transformers can also be used to interconnect balanced and unbalanced circuit sections.

DC Isolation

An RF transformer can also be designed to provide DC isolation between the primary and secondary windings, which can be useful for separating RF circuits that require a DC bias on the RF transmission line from RF circuits that would be negatively impacted by a DC voltage on the signal line.

Impedance Matching Transformer

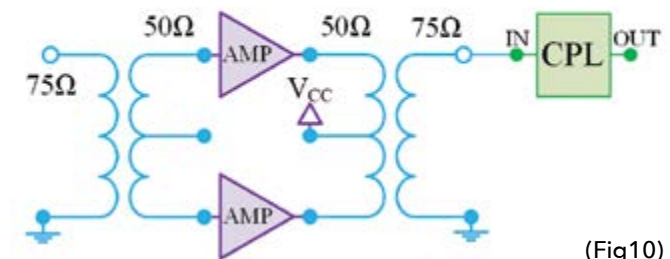


(Fig10)

Injecting DC Current

Moreover, if a DC current is required for a subsection of a circuit, a specialized RF transformer can be used to inject DC current into the signal path. For example, two center tapped transformers can be used to inject a DC bias, replacing the need for two Bias Ts (see Figure 11).

Replacing Two Bias Ts with Center Tap Transformers

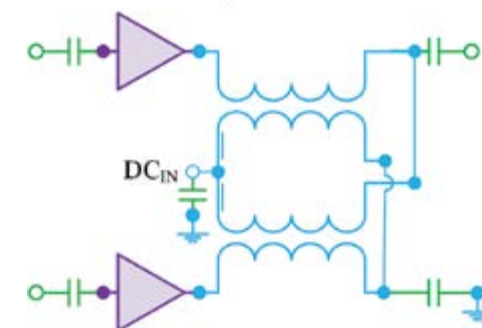


(Fig11)

Enhancing Common Mode Rejection

Certain RF transformer designs can be used to provide enhanced common mode rejection (CMR) for balanced (differential) circuits.

RF Choke

Other topologies can be used to filter high frequency RF components from a signal line, functioning as a choke.

CONCLUSION

RF transformers can be fabricated with a wide variety of manufacturing methods, with a diverse range of materials, and can be configured into a myriad of topologies in order to perform useful functions for RF circuits. Depending on the materials, construction, and design, RF transformers can be narrow- or wide-band, and operate at low RF frequencies or high. Understanding the basics, as well as more detailed nuances, of RF transformers can help a designer optimize a design with the right transformer selection.

This concludes Part 1 of the Demystifying RF Transformers Series. Stay tuned for the following articles:

Demystifying RF Transformers Part 2: Baluns & Ununs

Demystifying RF Transformers Part 3: Understanding RF Transformer Performance Parameters

Demystifying RF Transformers Part 4: How to Select the Ideal Transformer

RESOURCES

1. <https://www.minicircuits.com/app/AN20-001.pdf>
2. <https://www.minicircuits.com/app/AN20-002.pdf>
3. <https://www.minicircuits.com/appdoc/TRAN14-2.html>
4. RF and Microwave Transformer Fundamentals featured in Microwave Products Digest 10-2009
5. <https://www.minicircuits.com/WebStore/Transformers.html>



DESIGNER'S KITS

HIGHLIGHTS

- ▶ LTCC Designer's Kits for Wi-Fi, Bluetooth and Zigbee

To support customers working in Wi-Fi, Bluetooth and Zigbee applications, Mini-Circuits has developed a series of our popular LTCC filters and baluns optimized for the 2400 to 2500 MHz and 4900 to 5900 MHz bands. Two new designer's kits provide a selection of filters, duplexers, couplers and baluns for evaluation and prototyping.

2.4 to 2.5 GHz / 4.9 to 5.9 GHz

K1-LTCC-WBZ+
FILTERS / DIPLEXERS / BALUNS

- Perfectly suited for WiFi, Bluetooth & Zigbee applications
- Incredibly small sizes down to 0202
- LTCC robust construction
- Excellent Power Handling, Up to 2 Watts
- Low cost



K1-LTCC-WBZ+ Electrical Specifications (20 models, 5 of each, 100 Total)

	Model Number	Passband		Stopband 1		Additional Stopbands		Case Style
		(MHz)	Ins. Loss Typ. (dB)	(MHz)	Rejection Typ. (dB)	(MHz)	Rejection Typ. (dB)	
LOW PASS FILTERS	LPGE-592R+	4900-5900	0.7	9800-11800	42	14700-17700	54	GE0805C-4
	LPJC-592R+	4900-5950	0.4	8800-12600	49			JC0603C-1
	LPNK-252R+	2400-2500	0.5	4800-5000	42	7200-7500	40	NK0402C-1
	LPJC-252R+	2400-2500	0.5	4800-5000	52	7200-7500	34	JC0603C
	LPGE-252R+	2400-2500	0.3	4800-5000	44	7200-7500 9600-10000	40 37	GE0805C-2
HIGH PASS FILTERS	HPSC-492R+	4900-5900	0.4	500-2400	25	2400-2500	34	SC0202C
	HPJC-492R+	4900-5850	0.5	500-2400	25	2400-2500	36	JC0603C-7
	HPJC-252R+	2400-2500	1.0	500-1917	35	1917	25	JC0603C-4
BAND PASS FILTERS	BPNK-542R+	4900-5950	1.3	2400-2500	23	9800-11900 14700-17850	32 38	NK0402C-1
	BPJC-542R+	4900-5900	1.0	DC-2700	40	9800-12000	34	JC0603C-1
	BPGE-542R+	4900-5920	0.9	3500	49	9800-11840 14700-17760	32 30	GE0805C-3
	BPNK-252R+	2400-2500	3.3	695-800 1910	40 25	3200 4800-5000 7200-7500	36 23 22	NK0402C-1
	BPJC-252R+	2400-2500	2.3	695-800 1910	46 26	3200 4800-5000 7200-7500	38 29 43	JC0603C-1
BALANCED FILTERS	BPGE-252R+	2400-2500	1.3	1200-1300 2000	42 14	3000 3600-3800 4800-5000	18 43 37	GE0805C-3
	BFGE2-552R+	4800-5875	1.3	3500	49			GE0805C-2
	BFGE1-252R+	2400-2500	1.9	DC-1000 1000-2000	44 39	4800-5000 7200-7500	49 34	GE0805C-2
	BFNL2-252R+	2400-2500	1.7	880-960 1710-1910	59 38	4800-5000 7200-7500	42 32	NL1008C-2
DIPLEXERS	DPNK-252-492R+	2400-2500 5150-5850	0.4 1.2	700-2025 2400-2690 3500-3700 7250-7800 10300-11700	30 40 15 24 30	4800-6000 7200-7500	26 22	NK0402C
	DPJC-252-492R+	2400-2500 4900-5950	0.7 0.7	800-2500 9800-11900	34 37	4800-6000 7200-7500	28 28	JC0603C-3
	DPGE-252-492R+	2400-2500 4900-5950	0.4 0.5	800-2500 9800-11900	25 19	4800-6000 7200-7500	36 33	GE0805C-10

2.4 to 2.5 GHz / 4.9 to 5.9 GHz

K2-LTCC-WBZ+
COUPLERS / BALUNS

- Perfectly suited for WiFi, Bluetooth & Zigbee applications
- Incredibly small sizes down to 0402
- Rugged LTCC construction
- Excellent Power Handling
- Low cost



K2-LTCC-WBZ+ Electrical Specifications (21 models, 5 of each, 105 Total)

BALUNS	Model Number	Frequency Range (MHz)	Impedance Low (Ω)	Impedance Ratio	Case Style	Configuration		
	BLNK1-542R+	4900-5950	50	1	NK0402C	G		
	BLJC1-542R+	4900-5950	50	1	JC0603C	J		
	BLNK2-542R+	4900-5950	50	2	NK0402C	G		
	BLGE1-542R+	4900-5875	50	1	GE0805C-9	R		
	BLJC2-542R+	4900-5875	50	2	JC0603C	R		
	BLGE2-542R+	4900-5875	50	2	GE0805C-9	R		
	BLJC4-542R+	4900-5875	50	4	JC0603C	J		
	BLGE4-542R+	4900-5875	50	4	GE0805C-9	J		
	BLNK1-252R	2400-2500	50	1	NK0402C-1	S		
	BLJC1-252R	2400-2500	50	1	JC0603C	R		
	BLGE1-252R+	2400-2500	50	1	GE0805C-9	J		
	BLNK2-252R+	2400-2500	50	2	NK0402C	S		
	BLJC2-252R+	2400-2500	50	2	JC0603C	J		
	BLGE2-252R+	2400-2500	50	2	GE0805C-9	J		
BLJC4-252R+	2400-2500	50	4	JC0603C	J			
BLGE4-252R+	2400-2500	50	4	GE0805C-9	J			
COUPLERS	Model Number	Frequency Range (MHz)	Coupling Nom. (dB)	Mainline Loss (dB) Typ.	Directivity (dB) Typ.	VSWR (:1) Typ.	Power Input Max. (W)	Case Style
	CPJC-6-252R+	2400-2500	6.5	1.27	18	1.2	2	JC0603C
	CPJC-10-252R+	2400-2500	10	0.65	19	1.33	2	JC0603C
	CPJC-17-252R+	2400-2500	17.65	0.14	12	1.06	2	JC0603C
	CPJC-21-252R+	2400-2500	21	0.3	19	1.1	2	JC0603C
	CPJC-28-252R+	2400-2500	28	0.3	10	1.05	2	JC0603C



Direct Sales

- › **BROOKLYN**
sales@minicircuits.com
+1 718-934-4500
- › **MISSOURI**
sales@minicircuits.com
+1 417-335-5935
- › **EUROPE**
sales@uk.minicircuits.com
+44 1252-832600
- › **TAIWAN**
robert@min-kai.com.tw
+886 3 318 4450
- › **JAPAN & SOUTH KOREA**
thomasj@minicircuits.com
+81 45 548 5058

Technical Support

- › **NORTH AMERICA**
apps@minicircuits.com
+718- 934-4500
- › **SINGAPORE, INDONESIA
MALAYSIA, THAILAND**
sales@minicircuits.com.my
+604 646-2828
- › **ISRAEL**
app@ravon.co.il
+972 4 8749100
- › **TAIWAN & PHILIPPINES**
robert@min-kai.com.tw
+886 3 318 4450
- › **EUROPE**
apps@uk.minicircuits.com
+44 1252 832600
- › **INDIA**
apps@minicircuits.com
+91 44 2 2622575
- › **CHINA**
sales@mitron.cn
+86 591-8787 0001
Or
yuanzhong@minicircuits.com
+86 020-8734 0992
- › **JAPAN & SOUTH KOREA**
thomasj@minicircuits.com
+81 45 548 5058